✦✦ Scientific
✦✦ Research

Cracking of S235JR Cold-Deformed Steel during Galvanizing—Developing a Test to Evaluate and Predict the Effect of the Zinc Alloy Composition

Anne-Lise Cristol[1,2], David Balloy[1,2], Christophe Niclaeys[1,2], Philippe Quaegebeur[1,2], Ludovic Néel[3]

[1]Univ Lille Nord de France, Lille, France; [2]ECLille, Laboratoire de Mécanique de Lille, Villeneuve d'Ascq, France; [3]Galvazinc Association, Issy les Moulineaux, France.
Email: David.Balloy@ec-lille.fr

ABSTRACT

This paper presents a study on the cracking of steel pieces during their galvanization in alloyed liquid zinc. An experimental design was developed to show the effect of the amount of the various alloying elements (Sn, Bi, Pb) on this phenomenon. The characterization of the effect was obtained by 1) deformation by three-point bending of a piece of steel with different levels of deflection; 2) galvanizing and 3) observation and measurement of the cracks. A model of the critical deflection (deflection for crack starting) with the amounts of Sn, Pb, and Bi is presented and the predictions are described.

1. Introduction

The impact of atmospheric corrosion on resistance and aspect of steel structures is well known. The galvanization is one of the most usual ways to protect steel. Unfortunately, in some situations, steel cracks during hot-dip galvanizing. This phenomenon has been known for a long time. However, it has been insufficiently explored, and liquid metal-induced embrittlement (LME), grain boundary diffusion, or thermo-mechanical aspects could be, among other the possibilities, the cause.

LME has been the subject of many papers [1,2]. The mains studies are about the behavior of the steel in contact with liquid sodium [3-5] or Pb-Bi liquid alloys [6,7]. The case of steel in liquid zinc has only been studied in a few papers e.g. [8,9]. LME is the reduction in ductility and fracture stress of metals immerged in certain liquid metals [1,2,10,11], by reduction of the surface energy and a decrease of the critical stress intensity factor, K_{IC} [1,11].

The European FAMEGA program, which ended in 2007, studied the cracking of steel during galvanizing. Some parameters such as the steel grade, its surface treatments, the surface stress associated, pickling, fluxing, and the zinc alloy composition were studied. The results show that residual stresses induced by the steel forming lead to situations conducive to cracking [12,13] and that immersion in alloys of different compositions, including tin (Sn), bismuth (Bi), and lead (Pb), gives different resistance to cracking [14]. The effect of these elements on the thermal behavior of the bath has also been highlighted [15]. However, given the complexity of the phenomenon and the multitude of criteria, the underlying mechanisms have not yet been clearly demonstrated. Nonetheless, it is known that at least two conditions must be fulfilled for cracking. Firstly, the steel must have been strongly plastically deformed; secondly, it should have been immersed in a liquid metallic alloy [1,2].

In a previous work [16], we developed an experimental protocol (described in Section 2) to quantify the effect of the addition of Sn, Bi, and Pb to the galvanization bath on the cracking of steel specimens. This experimental work showed that the surface state of the steel influenced the test sensitivity. For an "as delivered" industrial state, the difference of the cracking behavior in two baths was greater than for a polished surface. In the latter case, for a given plastic deformation, no difference was observed for the tested compositions. In this protocol the samples are galvanized in conditions close to the industrial process.

This paper presents an experimental design performed to investigate the effect of the additions of Sn, Pb, and Bi in a galvanizing bath on the cracking of cold deformed steel, using our crack sensitivity test.

2. Experimental Procedure

2.1. Experimental Design

The chosen experimental design was the Roquemore 311B developed by K. G. Roquemore in 1976 [17,18]. The software that we used for applying the Roquemore 311B is MS Excel. It allows the study of the effects of three factors x_i (with i from 1 to 3) and allows the development of a quadratic mathematical model associated with a response surface y (Equation (1)). The response y of this experimental design is the minimal deflection that should be imposed on a steel sample for the appearance of cracks after galvanizing, here called "critical deflecttion." This cold deformation is performed on a steel sample using three-point bending.

The field of study is defined by the composition of the three alloying elements: Sn and Pb from 0 to 1 wt% and Bi from 0 to 0.1 wt%. The experimental design was associated with a mathematical model to estimate the simple interaction and the quadratic effects of the alloying elements as well as to provide an idea of the shape of the response surface in the field of study.

The experimental design contained 11 tests and defined the values taken by the factors x_i for each test (**Table 1**).

$$y = a_0 + a_1 x_1 + a_2 x_2 + a_3 x_3 + a_{12} x_1 x_2$$
$$+ a_{13} x_1 x_3 + a_{23} x_2 x_3 + a_{11} x_1^2 + a_{22} x_2^2 + a_{33} x_3^2 \quad (1)$$

with

a_0 the mean value of the response y; a_i the coefficient of the simple effect of the factor x_i; a_{ii} the coefficient of the quadratic effect of the factor x_i; a_{ii} the coefficient of the interaction effect of the factors x_i and x_j.

Table 1. Values of the factors x_i in the Roquemore 311B experimental design.

Test number	x_1	x_2	x_3
1	0	0	+2.449
2	0	0	−2.449
3	−0.751	−2.106	−1
4	+0.751	−2.106	+1
5	−0.751	+2.106	+1
6	+0.751	+2.106	−1
7	−2.106	−0.751	+1
8	+2.106	−0.751	−1
9	−2.106	+0.751	−1
10	+2.106	+0.751	+1
11	0	0	0

A factor x_i is related to a composition w_n of one of the studied elements: x_1, x_2, and x_3 are, respectively, related to the compositions w_{Sn}, w_{Pb}, and w_{Bi} of the galvanizing bath in the elements Sn, Pb, and Bi. For each element, a low and a high composition level (w_n^- and w_n^+) are defined. They correspond to the maximum and the minimum values of the composition of the elements tested (**Table 2**). For all the compositions, the low level w_n^- is equal to 0 wt%. The high level w_n^+ equals 1 wt% for w_{Sn}^+ and w_{Pb}^+, and 0.1 wt% for w_{Bi}^+.

Using the values of the factors, the low and high composition levels and the maximum and minimum values of the factors, the tested compositions can be calculated for the 11 tests (Equation (2)) and the experimental design matrix can be written (**Table 3**).

$$w_n = w_n^0 + s x_i \quad (2)$$

with

$$w_n^0 = \frac{w_n^+ + w_n^-}{2} \quad (3)$$

and

$$s = \frac{w_n^+ + w_n^-}{x_i^{max} - x_i^{min}} \quad (4)$$

Table 2. Low and high levels of element composition W_n (wt%).

	W_{Sn}	W_{Pb}	W_{Bi}
Low level	0	0	0
High level	1	1	0.1

Table 3. Experimental design matrix with Sn, Pb, and Bi composition (wt%).

Test number	W_{Sn}	W_{Pb}	W_{Bi}
1	0.500	0.500	0.100
2	0.500	0.500	0.000
3	0.321	0.000	0.039
4	0.678	0.000	0.070
5	0.321	1.000	0.070
6	0.678	1.000	0.039
7	0.000	0.321	0.070
8	1.000	0.321	0.039
9	0.000	0.678	0.039
10	1.000	0.678	0.070
11	0.500	0.500	0.050

The mean value and the sampling interval of the element composition.

2.2. Three-Point Bending Cold Deformation

The steel is a commercial hot rolled steel (EN 10025 -2 S235JR/AISI A36-04b/Y.S. = 235 MPa; A% = 21) of which the composition is given in **Table 4**. In agreement with the low carbon content, this steel is essentially constituted by ferrite grains with an average size of approximately 30 μm (**Figure 1**). The specimens with a $100 \times 20 \times 10$ mm^3 shape were extracted transversally in relation to the rolling direction from the $100 \times 10 \times 6000$ mm^3 plate. The surface of the sample was left unchanged.

Recent works [19,20] show that the cracking of steel depends on the rate of strain and there exists a critical stress leading to failure depending on the temperature of the liquid zinc.

In this study, the tests were performed according to the industrial treatment of pieces *i.e.* deformed at room temperature before galvanizing in liquid alloy at 450˚C. The cold deformation (at room temperature) was performed on steel samples using three-point bending on a 100-kN MTS electromechanical tensile machine equipped with a three-point bend bench (**Figure 2**). The bench had the following configuration: the two 25 mm diameter supports were 70 mm apart and the punch was 10 mm in diameter. The displacement of the punch was controlled at a rate of 50 mm/min.

For each test planned by the experimental design, various deflections from 12 to 32 mm were performed with three samples for each deflection.

Table 4. Composition of the steel (wt%).

| C	Mn	P	S	Si	Cu	Ni	Cr
0.043	0.546	0.007	0.021	0.133	0.315	0.090	0.113
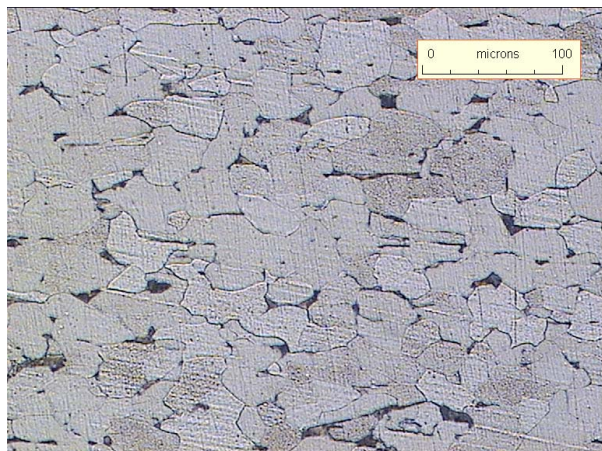
Figure 1. Micrograph of the steel.
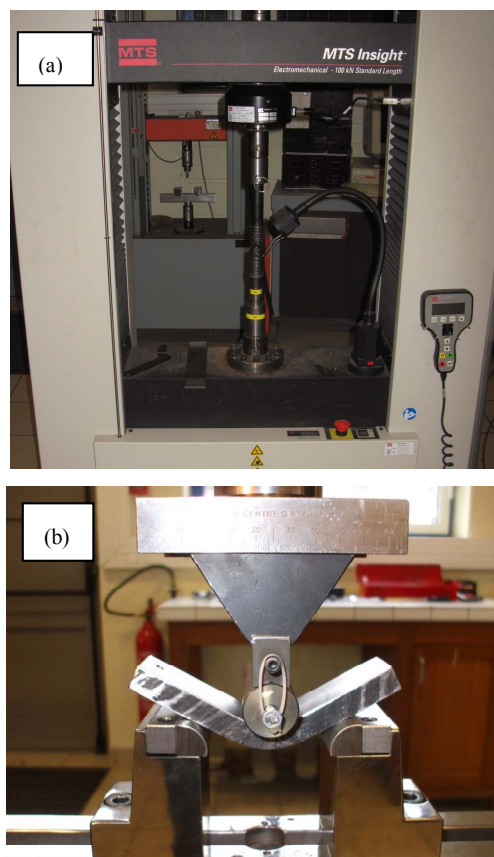
Figure 2. (a) MTS electromechanical tensile machine; (b) Three-point bend bench.

2.3. Galvanizing Process

After the three-point bending deformation, the samples were submitted to galvanizing (**Figure 3**).

The 11 baths planned in the experimental design were successively tested. The galvanizing baths were prepared for a total mass of 10 kg with respect to the compositions defined in **Table 3** and with an addition of 0.004 wt% of Al and 0.05 wt% of Ni and a saturation of Fe. Before galvanizing, the composition of the bath was checked using a LECO GDOES 850A spectrometer. Slight differences between the planned and performed compositions can appear. These differences were taken into account to correct the value of the factors that will be used to develop the mathematical model.

Before the anticorrosion treatment by galvanizing, the deformed steel samples underwent a preparation process composed of cleaning, pickling, and fluxing. The samples were cleaned for 30 min in a 2% Lerabilt®, provided by Stockmeier, (35% phosphoric acid + 20% sulfuric acid) in demineralized water and rinsed in water 2 min (30 s of immersion and 30 s of emersion ×2). They were then pickled 15 min in a bath composed of 150 g/L HCl + 60 g/L of Fe (427 g/L FeCl$_2$·4H$_2$O) + 0.2% Lera-

Figure 3. Galvanizing bath.

pas BP$^®$, provided by Stockmeier, (corrosion inhibitor: ethynylcarbinol alkoxylate 15% and but-2-yne-1,4-diol 5%) in demineralized water and rinsed 2 min as previously. Finally, they were prefluxed for 5 min in a bath of $ZnCl_2$ (220 g/L) - NH_4Cl (200 g/L) in demineralized water and dried at 110˚C for a minimal duration of 10 min.

The anticorrosion treatment was conducted by immersion of the steel samples in the liquid zinc alloy bath at 450˚C ± 2˚C (temperature controlled using a K-type thermocouple). The samples were immersed at a rate of 0.3 m/min, kept 3 min in the bath, and emerged at 0.3 m/min.

2.4. Definition of Critical Deflection

After the anticorrosion process, the samples were prepared for observation of the cracks. First, the samples were cut to extract the central part where the punch was located during the three-point bending test and then this central part was cut into two pieces (**Figure 4**). Each piece was embedded and then polished to a 6 μm grade. The presence of cracks was identified using an optical microscope (Olympus PMG3: **Figure 5**).

If cracks appeared, their length was measured. For each deflection of each bath composition tested, the total length of cracks (TLC) was calculated as the sum of the crack lengths measured on the two pieces of the three tested samples divided by 2.

For the 11 bath compositions, the TLC versus the imposed deflection could be plotted over time (**Figure 6(a)**). The curves were fitted using a third-order polynomial law and the value of the deflection at TLC = 0, called critical deflection, was determined (**Figure 6(b)**). This critical deflection value was the response that will be used in the experimental design.

3. Results

3.1. Response Surface

The values of factors x_i in the Roquemore 311B experi-
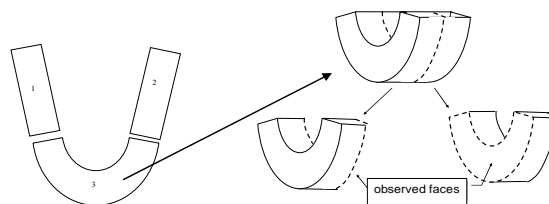

**Figure 4. Preparation of the samples for observation of cracks.**


Figure 5. Optical microscope (Olympus MPG3).
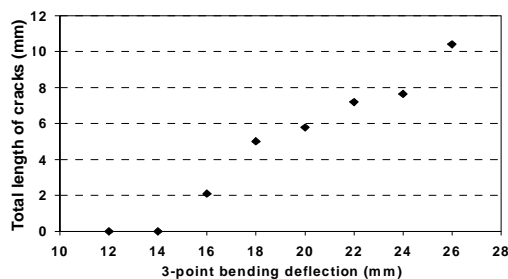
(a)
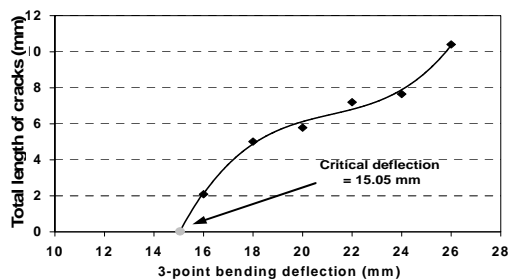
(b)

Figure 6. Total length of cracks at various deflections for bath no. (a) Raw results; (b) With the fitted 3rd-order polynomial law to determine the critical deflection.

Cracking of S235JR Cold-Deformed Steel during Galvanizing—Developing a Test to Evaluate and Predict the Effect of the Zinc Alloy Composition

79

mental design must be modified to take into account the effective compositions of the anticorrosion bath. The compositions measured before galvanizing are reported in **Table 5**. The modified values of the factors are calculated using Equation (2) and presented in **Table 6**.

The results of the tests in terms of TLC (**Table 7**) were used to determine the experimental design response *y*. Crack lengths range between 0.05 and 1.60 mm, and their number range from 0 to 8 for each level deflection. When the chemistry of the bath leads to a low level of cracking, few cracks with length < 0.8 mm are observed. Conversely, when the level of cracking is high the average length of cracks is 1.2 mm and their number rises up to 8.

Table 5. Composition of the baths (wt%).

Test number	Sn	Pb	Bi	Al	Ni	Fe	Zn
1	0.458	0.423	0.089	0.0035	0.0401	0.0229	98.964
2	0.430	0.420	<0.001	0.0044	0.0410	0.0460	99.058
3	0.307	0.005	0.038	0.0043	0.0501	0.0112	99.584
4	0.691	0.005	0.077	0.0039	0.0458	0.0196	99.158
5	0.340	0.926	0.056	0.0028	0.0437	0.0268	98.605
6	0.768	1.000	0.045	0.0031	0.0574	0.0195	98.107
7	0.014	0.342	0.090	0.0049	0.0586	0.0487	99.442
8	1.020	0.362	0.036	0.0043	0.0567	0.0246	98.496
9	0.014	0.667	0.045	0.0045	0.0575	0.0244	99.188
10	0.957	0.594	0.069	0.0032	0.0493	0.0196	98.308
11	0.500	0.433	0.045	0.0045	0.0474	0.0614	98.909

Table 6. Modified values of factors x_i.

Test number	X_1	X_2	X_3
1	−0.177	−0.324	1.912
2	−0.295	−0.337	−2.451
3	−0.813	−2.086	−0.588
4	0.805	−2.086	1.324
5	−0.674	1.795	0.294
6	1.129	2.107	−0.245
7	−2.048	−0.666	1.961
8	2.191	−0.582	−0.686
9	−2.048	0.707	−0.245
10	1.926	0.396	0.931
11	0.000	−0.282	−0.245

Table 7. Total length of crack in mm.

Test number	12	14	16	18	20	22
1	0	1.525	4.882	6.779	8.712	7.387
2	0	0	2.765	6.775	7.297	10.150
3		0	0	0.925	3.800	5.125
4		0	0	5.875	6.675	6.850
5	0	0	2.087	5.012	5.787	7.200
6	0	0.712	4.885	7.260	9.037	7.687
7	0	0	0	0.175	0	1.627
8	0	0.550	7.000	7.540	9.775	9.850
9			0	0	0	0
10	0	0	2.700	7.120	9.795	10.107
11	0	0	4.212	5.875	8.212	8.487

Test number	22	24	26	28	30	32
1	7.387					
2	10.150					
3	5.125	6.600	7.025			
4	6.850					
5	7.200	7.655	10.405			
6	7.687					
7	1.627	0.275	2.785	2.060		
8	9.850					
9	0	1.235	0	2.820	1	3.785
10	10.107					
11	8.487					

For each bath, the TLC values versus the three-point bending imposed deflection were plotted. **Figure 3(a)** shows an example of the results obtained for bath no. 5. No crack is observed for 12 and 14 mm deflections. The cracking phenomenon appears at a 16 mm deflection with a 2.1 mm TLC. The TLC reached 10.4 mm for the last deflection of 26 mm. To determine response y, some points were deleted from the curve: the points for TLC equals 0 and the points obtained for the last deflection if they presented stabilization behavior. For bath No. 5, points at 12 and 14 mm deflection were deleted. The last point obtained for a 26 mm deflection was retained since it did not show stabilization. The as-obtained curves were fitted using a third or second-order polynomial law according to the best convergence of points for *y* = 0. The response was determined as the value of the three-point

bending deflection at TLC equals 0 with the fitted curve. **Figure 3(b)** presents the fitted curve for bath No. 5. The response obtained for this bath was 15.05 mm. The experimental design matrix was completed with the response values (**Table 8**).

Using this matrix, the mathematical model associated with the experimental design can be developed as written in Equation (1). In this equation, the model is expressed as a function of the x_i factor values. As the value of the study is the influence of adding alloying elements, this model was rewritten to be expressed as a function of the w_n elements composition values (Equation (5)) using the relation between x_i and w_n presented in Equation (2).

$$\begin{aligned} y = b_0 &+ b_{Sn} w_{Sn} + b_{Pb} w_{Pb} + b_{Bi} w_{Bi} \\ &+ b_{SnPb} w_{Sn} w_{Pb} + b_{SnBi} w_{Sn} w_{Bi} + b_{PbBi} w_{Pb} w_{Bi} \quad (5) \\ &+ b_{SnSn} w_{Sn}{}^2 + b_{PbPb} w_{Pb}{}^2 + b_{BiBi} w_{Bi}{}^2 \end{aligned}$$

with

b_0 the mean value of the response y; b_n the coefficient of the simple effect of the element composition w_n; b_{nn} the coefficient of the quadratic effect of the factor w_n; b_{nm} the coefficient of the interaction effect of the factors w_n and w_m.

The mathematical model obtained for the experimental design is presented in Equation (6).

$$\begin{aligned} y = 25.99 &- 36.11 w_{Sn} - 1.38 w_{Pb} - 10.33 w_{Bi} \\ &+ 3.16 w_{Sn} w_{Pb} + 141.88 w_{Sn} w_{Bi} - 103.25 w_{Pb} w_{Bi} \quad (6) \\ &+ 19.58 w_{Sn}^2 + 3.62 w_{Pb}^2 - 201.80 w_{Bi}^2 \end{aligned}$$

According to the dimensional equation, the parameters unit is the same as y: mm. We assess the precision of y value +/− 1 mm.

Using this model, the surface response can be drawn to

Table 8. Complete matrix of the experimental design.

Test number	x_1	x_2	x_3	y
1	−0.177	−0.324	1.912	13.37
2	−0.295	−0.337	−2.451	14.75
3	−0.813	−2.086	−0.588	17.65
4	0.805	−2.086	1.324	15.95
5	−0.674	1.795	0.294	15.05
6	1.129	2.107	−0.245	13.75
7	−2.048	−0.666	1.961	20
8	2.191	−0.582	−0.686	13.8
9	−2.048	0.707	−0.245	22.2
10	1.926	0.396	0.931	15.2
11	0.000	−0.282	−0.245	14

study the simple interaction and quadratic effects of the alloying elements.

3.2. Analysis of the Results of the Mathematical Model

The a_i coefficient of the mathematical model should represent the simple and combined effects of the alloying elements. However, this model allows the prediction of the critical deflection (CD) as a function of the chemical composition of the bath alloy, but the parameters a_i result only from a mathematical treatment of the results and are not representative of a physical phenomenon. Moreover, from the a_i coefficients it is not possible to conclude on the behavior of the CD with the contents of the alloying elements. However, it is possible to present the results in terms of CD vs. the chemical composition.

3.2.1. Effect of Pb and Bi with Constant Sn wt%
Figure 7 presents a two-dimensional representation of the CD for the iso Sn contents (0, 0.5 and 1 wt%). When the zinc alloy wt% Sn equals 0, the CD varied from 30 mm (less sensitive to cracking) to 14.9 mm (more sensitive to cracking). In the corner near (0.1 wt% Bi and 1 wt% Pb), the CD is the lowest (14.85 mm). In the corner near (0 wt% Bi and 1 wt% Pb), the CD is the highest (28.23 mm).

Also, when there was no Sn in the galvanizing bath, addition of lead slightly decreased the sensitivity to cracking. Without Pb, the addition of Bi slightly increased the sensitivity to cracking. When the two elements were added simultaneously, there was a more significant decrease in CD.

When the Sn content rose to 0.5 wt%, the CD decreased. The Bi + Pb-rich corner was still the zone where the CD was the lowest, with a value calculated for 1 wt% Pb and 0.1 wt% Bi equal to 10.6 mm. Here, the central area was trough-shaped, with a CD lower at the center than in the corners, which were rich only in Bi or in Pb. For example, for (0.05 wt% Bi, 0.5 wt% Pb) CD = 13.95 mm, for (0.1 wt% Bi , 0 wt% Pb) CD = 17.04 mm, and for (0 wt% Bi , 1% Pb) CD = 16.79 mm.

When the Sn content rose to 1 wt%, the area with the lowest CD was displaced to the corner (0 wt%Bi, 0 wt% Pb). The CD increased with the Bi and the Pb content, and the CD is maximal in the corner (0.1 wt% Bi , 0 wt% Pb).

3.2.2. Effect of Sn and Bi with Constant Pb wt%
Figure 8 shows a two-dimensional representation of the CD for iso Pb contents (0, 0.5 and 1 wt%). Without Pb and Bi in the galvanizing bath, the CD increased with the Sn content. This means that cracking will appear for a less damaged steel when the Sn content increases. Be-
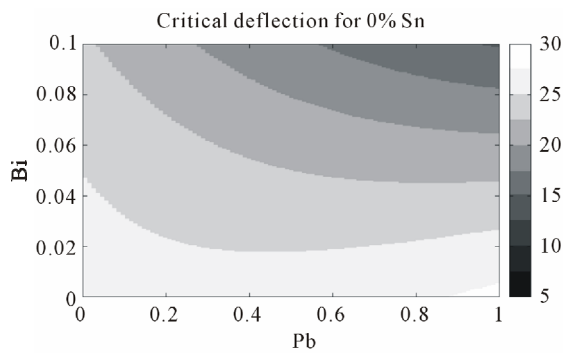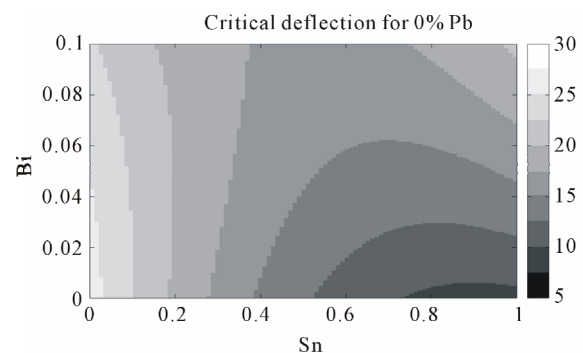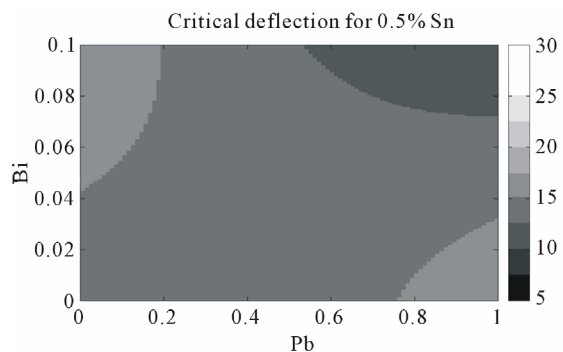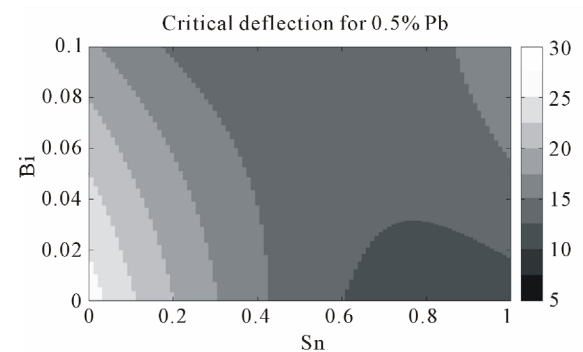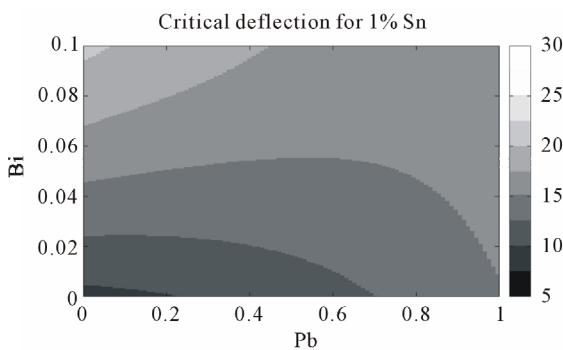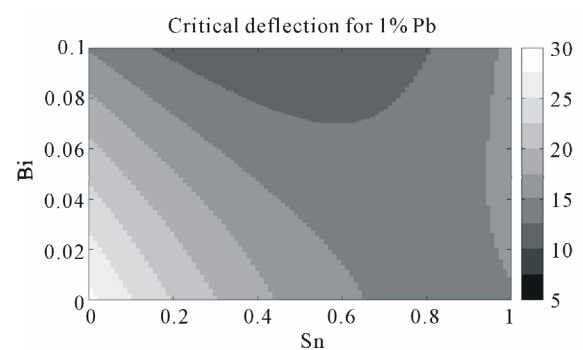
Figure 7. Two-dimensional representations of the critical deflection with constant wt% Sn content: (a) 0%; (b) 0.5; (c) 1%.

Figure 8. Two-dimensional representations of the critical deflection with constant wt% Pb content: (a) 0%; (b) 0.5%; (c) 1%.

tween 0 and 0.06 wt% Bi, the CD demonstrated the same behavior when the Sn content rose. For %Bi higher than 0.06 wt%, the CD vs % Sn presents a minimal value. The corners (0.1 wt% Bi, 1 wt% Sn) with CD = 20.66 mm and (0.1 wt% Bi, 0 wt% Sn) with CD = 22.90 mm were less sensitive to cracking than the central position (0.06 wt% Bi, 0.6 wt% Sn) CD = 15.31 mm. Adding Bi increased the CD (beneficial effect) when the Sn content was high, whereas it decreased the CD when Sn content was low.

When Pb content increased to 0.5 wt%, the positions of the areas with the highest CD (0 wt% Bi, 0 wt% Sn)

and (0.1 wt% Bi, 1 wt% Sn) and those with the lowest CD (0 wt% Bi, 1 wt% Sn) remained more or less the same, with a central trough of a lower CD.

With 1 wt% Pb, the more at-risk area shifted upwards (0.1 wt% Bi, 0.6 wt% Sn), and in these conditions, the lower the Sn and Bi contents, the higher the CD. Thus, cracking sensitivity is lower.

3.2.3. Effect of Pb and Sn with Constant Bi wt%

Figure 9 shows a two-dimensional representation of the CD for iso Bi contents (0, 0.05 and 0.1 wt%). Without Pb and Bi in the galvanizing bath, the CD decreased

(a)

(b)

(c)
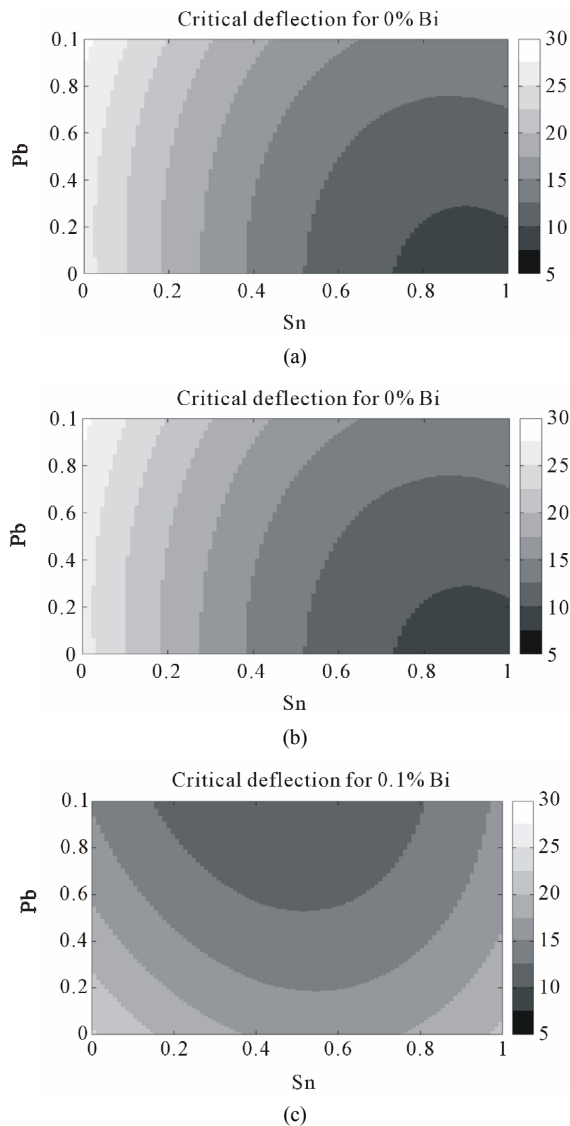
Figure 9. Two-dimensional representations of the critical deflection with constant wt% Bi content: (a) 0%; (b) 0.05%; (c) 0.1%.

drastically with the increase of Sn from 25.9 mm for 0 wt% Sn to 9.65 mm for 1 wt%. This means that the sensitivity for cracking is higher when the Sn content increases. When the Pb content increased, without Sn, the CD increased (less cracking). In the presence of Sn, the CD was higher when Pb was added. This shows the beneficial effect of the addition of Pb.

For Bi wt% = 0.05, the cracking sensitivity was globally better. The lowest level was around 15 mm. The adverse effect on CD of an increase of Sn content remains, but the beneficial effect of Pb disappears.

When 0.1 wt% Bi was added to the bath, the most critical area is displaced to the center and the top of the graph. In these conditions, the addition of Pb decreased

CD, which means that cracking sensitivity increases. The first addition of Sn—between 0 and 0.5 wt% Sn—decreased CD, but with a second addition—between 0.5 and 1 wt% Sn—the CD increased.

3.2.4. Discussion on the Mathematical Model

The results of this study are in agreement with the study [21]. The **Table 9** presents a comparison between the results of [21] and the results of the same bath compositions calculated with the mathematical model presented in this paper.

When the chemical bath composition leads to a low strain to failure (ε_f) according to [21], as for the bath named a_2, the CD calculated with the model proposed is low. For compositions a_0 and a_1, the evolutions of ε_f and CD are correlated.

The model obtained with the experimental design shows the best precision when the compositions within the area defined by the experimental compositions tested. Outside the area defined, results may be less reliable. The further we depart from this experimental data, less reliable the results will be.

4. Conclusions

This paper presents a study on the measurement of the sensitivity to cracking of steel parts during their galvanization in alloyed liquid zinc, to improve corrosion resistance.

Using a protocol defined in a previous work [16] to measure the number and length of cracks formed on steel during the anticorrosion process, an experimental design was carried out to study the effect of the chemical composition of the zinc alloy on steel cracking. The influence of Sn, Pb, and Bi contents was studied. A model to predict the critical deflection y, *i.e.* the minimum deflection to observe cracks on steel after galvanization, versus the amounts of Sn (w_{Sn}), Pb (w_{Pb}), and Bi (w_{Bi}) is proposed:

$$y = 25.99 - 36.11w_{Sn} - 1.38w_{Pb} - 10.33w_{Bi}$$
$$+ 3.16w_{Sn}w_{Pb} + 141.88w_{Sn}w_{Bi} - 103.25w_{Pb}w_{Bi}$$
$$+ 19.58w_{Sn}^2 + 3.62w_{Pb}^2 - 201.80w_{Bi}^2$$

The coefficients do not have a physical signification, but result from a mathematical treatment of numerical data. As a consequence, it is not possible to draw a con-

Table 9. Comparison between [21] and this study.

Bath [21]	wt% Sn	wt% Pb	wt% Bi	ε_f (%)	CD (mm)
a_0	1.20	0.00	0.10	10	18
a_1	0.00	0.70	0.00	31	>22
a_2	1.00	1.10	0.05	6	16

Cracking of S235JR Cold-Deformed Steel during Galvanizing—Developing a Test to Evaluate and Predict the
Effect of the Zinc Alloy Composition

83

clusion concerning the effect of only one element regarding its coefficients. Indeed, this work highlights the fact that the interaction of these 3 elements has a strong impact on the behavior of the room temperature deformed steel during anticorrosion treatment. This model allows the drawing of 2D diagrams showing the variation of y versus two of the three elements and with the third fixed. As examples, these tendencies are commented on.

REFERENCES

[1] M. G. Nicholas and C. F. Old, "Liquid Metal Embrittlement," *Journal of Materials Science*, Vol. 14, No. 1, 1979, pp. 1-18. doi:10.1007/BF01028323

[2] H. Nies, G. Schambil and B. Stiefel, "The Problems Associated with the Cracking in Hot-Dip-Galvanised Steel Structures," *Welding and Cutting*, No. 5, 2007, pp. 256-260.

[3] P. Skeldon, J. P. Hilditch, J. R. Hurley and D. R. Tice, "The Liquid Metal Embrittlement of 9Cr Steel in Sodium Environments and the Role of Non-Metallic Impurities," *Corrosion Science*, Vol. 36, No. 4, 1994, pp. 593-610. doi:10.1016/0010-938X(94)90066-3

[4] J. P. Hilditch, J. R. Hurley, P. Skeldon and D. R. Tice, "The Liquid Metal Embrittlement of Iron and Ferritic Steels in Sodium," *Corrosion Science*, Vol. 37, No. 3, 1995, pp. 445-454. doi:10.1016/0010-938X(95)92861-E

[5] O. Hamdane, J. Bouquerel, I. Proriol-Serre and J. B. Vogt, "Effect of Heat Treatment on Liquid Sodium Embrittlement of T91 Martensitic Steel," *Journal of Materials Processing Technology*, Vol. 211, No. 12, 2011, 2085-2090. doi:10.1016/j.jmatprotec.2011.07.006

[6] D. Sapundjiev, S. Van Dyck and W. Bojaerts, "Liquid Metal Corrosion of T91 and A316L Materials in Pb-Bi Eutectic at Temperatures 400 - 600˚C," *Corrosion Science*, Vol. 48, No. 3, 2006, pp. 477-594. doi:10.1016/j.corsci.2005.04.001

[7] A. Legris, G. Nicaise, J. B. Vogt, J. Foct, D. Gorse and D. Vançon, "Embrittlement of a Martensitic Steel by Liquid Lead," *Scripta Materialia*, Vol. 43, No. 11, 2000, pp. 997-1001. doi:10.1016/S1359-6462(00)00523-6

[8] J. Carpio, J. A. Casado, J. A. Alvarez, D. Mendez and F. Gutierrez-Solana, "Stress Corrosion Cracking of Structural Steels Immersed in Hot-Dip Galvanizing Baths," *Engineering Failure Analysis*, Vol. 17, No. 1, 2009, pp. 19-27. doi:10.1016/j.engfailanal.2008.11.005

[9] J. Carpio, J. A. Casado, J. A. Alvarez and F. Gutierrez-Solana, "Environmental Factors in Failure during Structural Steel Hot-Dip Galvanizing," *Engineering Failure Analysis*, Vol. 16, No. 2, 2009, pp. 585-595.

doi:10.1016/j.engfailanal.2008.02.006

[10] P. J. L. Fernandes and D. R. H. Jones, "The Effect of Temperature on Fatigue Crack Growth in Liquid Metal Environments," *Corrosion Science*, Vol. 38, No. 5, 1996, pp. 745-754. doi:10.1016/0010-938X(95)00163-E

[11] Y. J. Su, Y. B. Wang and W. Y Chu, "Chemisorption-Facilitating Dislocation Emission, Multiplication and Motion," *Scripta Materialia*, Vol. 36, No. 11, 1997, pp. 1239-1244. doi:10.1016/S1359-6462(97)00020-1

[12] B. Donnay, "Failure Mechanisms during Galvanizing," *Proceedings of the European General Galvanizers Association*, Edinburgh, 10-14 June 2007.

[13] T. Pinger, "Failure Mechanism during Galvanizing (FAMEGA)—Modelling," *Proceedings of the European General Galvanizers Association*, Edinburgh, 10-14 June 2007.

[14] A. Völling, W. Bleck, M. Feldmann and P. Langenberg, "FAMEGA: Laboratory Testing of Zinc Alloys," *Proceedings of the European General Galvanizers Association*, Edinburgh, 10-14 June 2007.

[15] S. W. Wen and B. Rudd, "Modelling Analysis of Stress and Strain during Hot-Dip Galvanizing," *Proceedings of the European General Galvanizers Association*, Edinburgh, 10-14 June 2007.

[16] D. Balloy, A.-L. Cristol, C. Niclaeys, P. Quaegebeur and L. Néel, "Experimentation and Modeling of Thermo-Mecanical Phenomena That Appear during Hot Dip Galvanizing," *Proceedings of the International Galvanizing Conference and Exhibition*, 22nd, Madrid, 8-12 June 2009.

[17] J. Goupy, "Plans D'expériences Pour Surface de Réponse," In: D. K. G. Roquemore, *Technometrics*, Vol. 18, 1976, pp. 419-424.

[18] K. G. Roquemore, "Hybrid Designs for Quadratic Response Surfaces," *Technometrics*, Vol. 18, No. 4, 1976, pp. 419-424. doi:10.1080/00401706.1976.10489473

[19] C. Beal, X. Kleber, D. Fabregue and M. Bouzekri, "Embrittlement of a Zinc Coated High Manganese TWIP Steel," *Materials Science and Engineering*: A, Vol. 543, 2012, pp. 76-83. doi:10.1016/j.msea.2012.02.049

[20] C. Beal, X. Kleber, D. Fabregue and M. Bouzekri, "Liquid Zinc Embrittlement of Twinning-Induced Plasticity Steel," *Scripta Materialia*, Vol. 66, No. 12, 2012, 1030-1033. doi:10.1016/j.scriptamat.2011.12.040

[21] M. Feldmann, T. Pinger, D. Shäfer, R. Pope, W. Smith and G. Sedlacek, "Hot-Dip-Zinc-Coating of Prefabricated Structural Steel Components," *Joint Report Number EUR* 24286. *JRC-ECCS Cooperation Agreement for the Evolution of Eurocode* 3, 2010.